13th World Conference on Earthquake Engineering
Vancouver, B.C., Canada
August 1-6, 2004
Paper No. 2735

DAMAGE IDENTIFICATION OF STEEL SQUARE TUBULAR COLUMNS UNDER EARTHQUAKE LOADING

Y.S. PARK[1], S.Y. HAN[2], B.C. SUH[3], H.J. HONG[4] and Y.B. JEON[5]

SUMMARY

This study proposed a damage identification for steel members and examined a process which steel square tubular columns under seismic loading reach a failure with the damage index. Using a finite element program, a nonlinear analysis was carried out and a damage process was analyzed. Material properties and strain characteristics were obtained from material testing. This study uses the connection of the material composition of the bilinear stress-strain to develop an analysis technique applying the damage index and interprets the character of material in a plastic domain as bilinear kinematic hardening. An effect on the damage of members was analyzed by varying kinds of steels and conditions of loading based by the material test results. The steel types are applied to a general structure type-rolled steel material SS400 and a high-tensile steel material Posten 80. Loading conditions are as follows; an steady increase load of a tension domain in the state of a center axis compression load, an alternating fixed displacement of a tension domain in the state of a center axis compression load, an alternating steady increase displacement of a tension-compression domain in the state of a center axis compression load. According to the strain characteristics and cumulative plastic strain about each variable, the effect on the damage by conditions of loading and kinds of steels was able to be estimated quantitatively.

INTRODUCTION

Introductory material Buildings, bridges, and other civil engineering structures must resist hundreds of loading cycles caused by strong earthquakes, while major damage can occur with as few as 30 cycles of large plastic deformations. Past studies using experiments on steel structural members, including columns, beams and braces, commonly report that global buckling of steel members can easily trigger local buckling of thin-plate elements[1]. The local buckling causes concentrated large plastic deformations, which within five to 20 loading cycles induce cracking that eventually leads to rupture of the members. Also, it has been observed that seismic loading of steel members has caused ruptures at local buckling locations[11].

[1] Professor, Chonnam National University, Gwangju, Korea. Email : parkys@chonnam.ac.kr
[2] Graduate Student, Chonnam National University, Gwangju, Korea. Email : janari@hanmail.net
[3] Part-time Teacher, Chonnam National University, Gwangju, Korea.
[4] Graduate Student, Chonnam National University, Gwangju, Korea.
[5] Graduate Student, Chonnam National University, Gwangju, Korea.

Some of previous researchers have classified this type of failure as low-cycle fatigue. However, fatigue generally means a failure caused by crack propagation without macroscopic deformations. Therefore, classifying failures that occur under repeated large deformations, such as those in this study, as belonging the category of fatigue failure is questionable. It is proposed that this phenomenon should be called very low cycle failure[3].

As was indicated before, to investigate the cracks of the failed structural members under the condition of cyclic loading, it is necessary to examine both the overall behavior of the members and the local behavior of member portions where cracks are generated. However, no research has combined this overall and local behavior of the structural members under cyclic loads so far. The main purpose of this study is to suggest a comprehensive explanation in regard to damage behavior and to acquire basic information for damage evaluation of steel structures when they are subject to earthquakes.

First, the damage behavior of steel members was examined when they experience repetitive plastic deformation and finally reach failure. Then, the factors that influence these behaviors were classified and analyzed. Third, a new damage index equation was suggested according to the results of this analysis.

In addition, a finite element analysis using variables of loading patterns and steel types was carried out to investigate the deformation pattern, stress-strain hysteresis and stress of steel members that are subject to certain types of cyclic loads.

DAMAGE EVALUATION

Fatigue Problems of Plastic Structural Members under Cyclic Loading

Several experimental studies have been carried out to investigate the stability strength characteristics of steel structures such as columns, beams and bracings under the condition of cyclic loading. The results of these studies have suggested that the cyclic load causes overall buckling that is accompanied by local buckling, and that the plastic deformations that are caused by local buckling grows into cracks, which entail the failure of the structural members. Furthermore, this result is verified from several earthquake field reports showing that the failure of steel structures occurred where there was local buckling. This kind of failure results from varying stress distribution of the steel members and has the following characteristics.

First, the failure does not show any apparent deformations and only cracks on the steel members develop. In the meantime, the failure surface is very smooth. Secondly, the relationship between the repetition number N and stress amplitude S can be represented as the following general S-N curves or Wohler curves in Eq. (1) and (2).

$$S = AN^{-m} \tag{1}$$

$$S = a - b\log N \tag{2}$$

Here *A, m, a, b* are integers.

The third characteristic of this kind of failure is that the deviation of *N* is relatively large for a certain value of *S*. Therefore, dealing with the failure of the steel members which behave within the zone of plastic deformation under cyclic loading patterns is not very reasonable.

Under strong earthquakes, the elastio-plastic response number of a structure can be recorded more than a hundred times, but the response number of plastic deformation that is directly related to the damage of the structure is not high. Thus, to figure out the nature of crack generation within the range of small repeated numbers, it is necessary to examine both the overall behavior of the members and the local behavior of member portions where cracks are generated.

The failure and damage behavior of structures are generally governed by the combination of physical properties such as stress and strain, chemical properties such as corrosion and the characteristics of the materials that are used in the structure[8]. The types of failures that are considered to be problematic to structures include (1) brittle failure, an instantaneous failure that is caused by micro-scale defects or cracks in the structure, (2) ductile failure, which occurs when cracks that are generated by an increase in

load or strain lead a structure into plastic unstable breaking, (3) fatigue failure, which is caused under cyclic loading patterns, (4) stress corrosion failure and (5) creep failure.
The fatigue strength of an individual structural member can be represented by the well-known S-N curve. This S-N curve shows very complicated behaviors, and it can change with various factors such as the external conditions of steel, including defects, sizes, surface treatment status and the surrounding environment, as well as internal conditions including the physical and chemical properties of the material and the heat treatment method that is applied to it. For general mild steel, the fatigue where the cycle is less than 10^4 is regarded as low-cycle fatigue or plastic fatigue. In this case, the life evaluation is usually performed on the basis of the strain of the material.
No research has yet been focused on the failure of steel structures caused by several tens or hundreds of cyclic loads. The cyclic bending behavior of structural members under a certain displacement amplitude can be classified into two cases where the hysteresis loop is normalized or where the hysteresis loop is deteriorated. The latter is related to the local deformation and instability of steel members. In this case, the steel members tend to fail sooner than expected[13]. If the axial force exists, the behavior becomes more active. According to the results of these studies, the relationship between the load displacement amplitude and the cycle number of failure can generally be represented as straight lines with a negative slope in log-log scale plots.
However, a definition for failure has not been unified, and is still under debate among many researchers. The load that is applied on the real structures does not have certain amplitude and is actually a very irregularly varying load with various means and amplitudes. The fatigue strength under cyclic loads varies not only with frequency but also with the sequence of the applied load.
Many theories and methods have been suggested for the evaluation and analysis method of fatigue life and damage of the steel structures that are subject to irregular cyclic loads, but no theory or method has been verified sufficiently to be used as a unified standard. The major reason for that is that the related studies have focused primarily on the experimental aspect of this natural phenomenon, and the fatigue fracture mechanism has not yet been fully examined. Also, earthquakes are statistically very uncertain phenomena, which make close examination even more difficult.

Damage Evaluation of Steel Structures under Cyclic Loading

The damage degree for steel structure members that are subject to severe cyclic loading can be evaluated as follows. Firstly, the cumulative plastic strain is calculated for each cycle of the load. Then, this value is compared to the ultimate local strain that is obtained from the failed portion of the steel specimen which went through the tension test. If the cumulative plastic strain at the section where the stress concentration was the highest exceeds the ultimate strain at the rupture, the material is defined to have failed. Thus, the damage index of steel structures under cyclic loads such as a strong earthquake load can be represented in Eq. (3) and (4).

$$If \sum_{i=1}^{n} \varepsilon_i \geq \varepsilon_{\lim} \text{ , then failure state} \tag{3}$$

$$If \sum_{i=1}^{n} \varepsilon_i < \varepsilon_{\lim} \text{ , then no failure} \tag{4}$$

Here, N is the cycle number,
ε_i is the local strain at the element with the highest stress concentration
ε_{lim} is the limit local strain at the rupture
Thus, the damage degree D up to N cycle can be quantified in Eq. (5).

$$D = \sum_{i=1}^{n} \left(\frac{\varepsilon_i}{\varepsilon_{\lim}}\right) \tag{5}$$

If D is equal to or less than 1, this means the steel material has failed at the corresponding loading cycle. Conversely, if the D value is smaller than 1, this means the steel material has not failed. It also numerically shows the degree of the damage on the steel material.

DAMAGE DEGREE EVALUATION USING FINITE ELEMENT METHOD ANALYSIS

Material Test and Assumptions in Analysis

The stress-strain curve was obtained from the tension test. From this test, the essential mechanical properties of steel such as proportional limit, elasticity limit, yield point, yield strength, Youngs modulus and tensile strength were acquired. Also, this test could evaluate elongation, reduction of area from the investigation of shapes and sizes of the failed specimens.

This study used the relationship between Young's modulus and the E_t, and the relationship between nominal yield stress and strain as a material property by idealizing it bilinear as shown in Fig. 1. Uniaxial stress strain relationship, Young's modulus and Poisson's ratio ν for the plasticity zone are given in Table 1. Also, the Von Mises Failure condition was used.

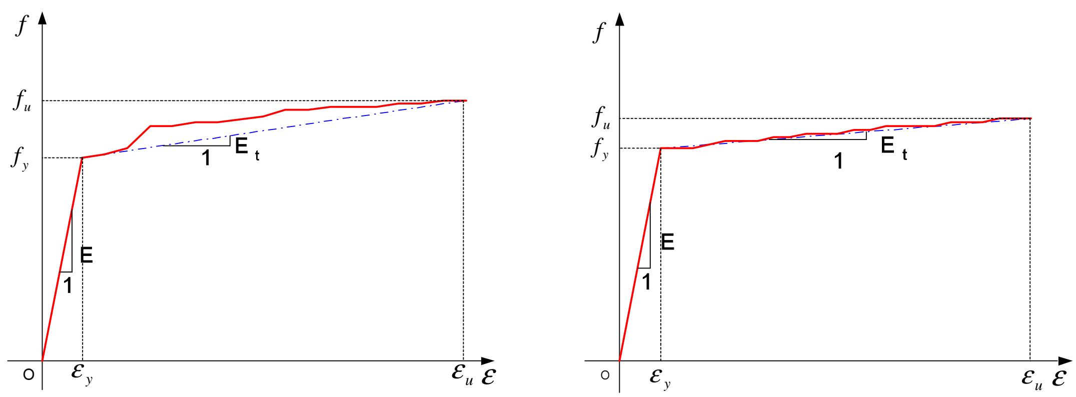

(a) SS400 (b) Posten80

Fig. 1 Strain-Stress Relation

Table. 1 Material Property

Specimen	F_y (kgf/cm^2)	F_u (kgf/cm^2)	E_t (kgf/cm^2)	E (kgf/cm^2)	E_t/E	Material Type
US40-*	3478	3751	1792.35	1987301.71	9.02×10^{-4}	SS400
US80-*	6694	6889	3630.45	2018831.12	1.80×10^{-3}	Posten80
Note : ν=0.3, * = All inclusion of attached name						

In general, the analysis precision of a member hysteresis behavior is primarily governed by the material constituent. Also, for the analysis within the range of strain hardening, the precise modeling of the material constituent is necessary.

This study investigated the relationship between the cyclic stress and the strain of the steel material in the strain zone, and the bilinear stress-strain relationship for the development of an analysis method that takes advantage of the damage index was chosen. Furthermore, an analytical approach was used assuming bilinear kinematic hardening as a property of steel material in the plasticity zone[9]. Thus, it can be more easily noticed the degree of damage because the stress-strain relationship is not exponential but linear. The following to apply the damage index that this study suggests was assumed. This assumption represents the idealistic elasto-plastic behavior of the material.

1. The upper yield point is ignored. - Since almost all of the steel material does not have the upper yield point, this assumption is reasonable.

2. The zone of strain hardening is ignored. - Most steel materials show the zone of strain hardening when they reach failure, so this assumption can induce errors. However, as seen from the stress-strain curve, the slope of that is small, and the strength of the material increases in the zone of strain hardening, which means a little more safety can be obtained from this assumption. Possible errors might occur, but the amount is insignificant enough to be ignored.
3. The Bauschinger effect is ignored. - the error that this assumption can induce is insignificant enough to be ignored too.
For more precise analysis, the hysteresis constituent modeling that includes uni-directional hardening will be necessary.
Fig. 2 shows the strain after the break of a specimen in the tension test. The SS400, which is standard-strength cold drawn steel for structures, showed 150% of the maximum strain at the rupture, while the high-strength Posten80 showed 130% of the maximum strain. As for the strain distribution, the strain of the Posten80 was concentrated in the portion where the failure took place, while the SS400 strain was rather evenly distributed along the length of the specimen tested.

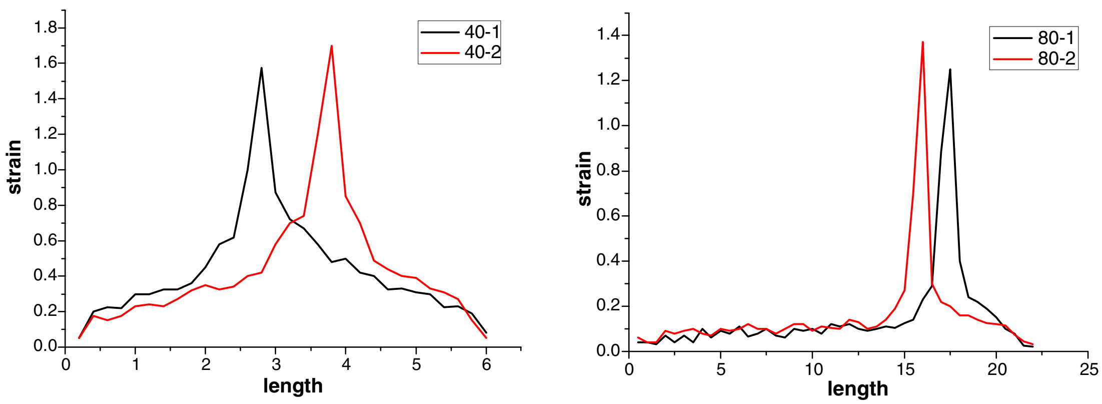

(a) SS400 (b) Posten80

Fig. 2 Strain Distributions in Test Specimen

Finite Element Modeling

Geometric non-linear analysis was carried out using a box-shaped steel member to develop an analysis method for steel members that are subject to severe cyclic loads. The box shaped steel member was designed to go through overall buckling accompanied by local buckling, and then show large plastic deformation with the application of cyclic loading. This kind of elastic and plastic behavior can be traced out using the finite element method that considers non-linearity material and geometric non-linearity. In this analysis, a structural analysis program, sol106 of MSC/NASTRAN version 70.7.2 was used.
Fig. 3 shows the finite element model and the basic coordinate system of the box-shaped steel member that is used in this study. The box-shaped B-210x210x9 was chosen. The model is fixed at one end and hinged at the other end. It freely rotates with respect to the Y-axis that penetrates the model from top to bottom. The length, *h* of the model is 1000mm.
The QUAD4, which is a shell-plate one-directional tetragon element, was used in the structural model, and triangular elements, the TRIA3 were used near each edge of the model where loads were applied. In the one directional element, the function that represents the shape of the element and the displacement function is the same. In this case, the coordinate transformation and displacement function have exactly the same transformation. This kind of element can be applied in the modeling of thick shells and non-linear material since the stress in the direction of thickness can be evaluated when the material is subject to bending. In QUAD4, strain and curvature were assumed to vary linearly, and in TRIA3, strain and curvature were assumed to be constant[10]. This model consists of 616 elements. The model was divided into 22 pieces in the longitudinal direction, and was also divided into 7 pieces for all 4 sides of the

member in the direction that is perpendicular to the Y axis. The element separation of the model was performed considering the condition such as local strain to closely investigate the behavior of the member such as overall buckling and local buckling.

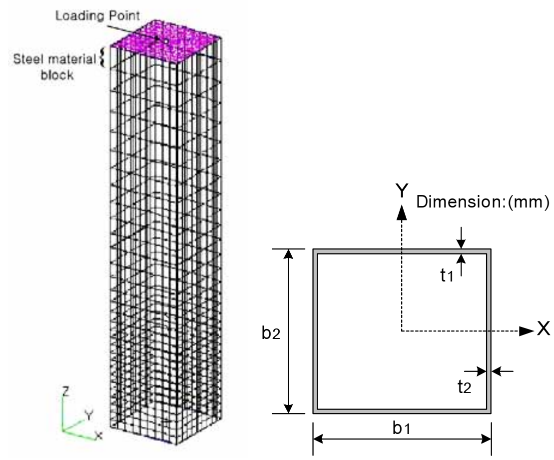

Fig. 3 Model for Analysis

Table. 2 Model Size and Identification

US 40 - 32 - 69 - CL

US: Unstiffened Steel Members
40: Material Type (40: SS400, 80: Posten80)
32: $\bar{\lambda}$
69: R
CL: Loading Pattern (LL: Lateral Load, CD: Constant Displacement Cycles, RD: Fully Reversed Displacement Cycles)

Length h (mm)	Width $b1$ (mm)	Width $b2$ (mm)	Thickness t (mm)
1000	210	210	9
Section Area A (mm^2)	Rotation radius r (mm)	Width-thickness ratio b/t	Slenderness ratio λ
7236	82.14	23.33	29.22

In general three-dimensional analysis, each node displacement has 6 degrees of freedom, but in the case where the stiffness is not defined for the rotation with respect to the tangent line of the plate element, or in the part of analysis of forced blocks by rotation restraint, modulus of elasticity and yield strength are set to a large value and they can only have 5 degrees of freedom. Names and sizes of the model are shown in Table 2.

$\bar{\lambda}$ is the slenderness ratio parameter of a compression member in Eq. (6).

$$\bar{\lambda} = \frac{1}{\pi}\sqrt{\frac{F_y}{E}}\left(\frac{l_e}{r}\right) \tag{6}$$

Here, E is the young's modulus, l_e is effective buckling length (K_l and K are effective buckling length coefficients (2.0 for fixed end compression members)) and r is the radius of rotation.

R is the equivalent width-thickness ratio parameter of plates in Eq. (7).

$$R = \frac{1}{\pi}\frac{b}{t}\sqrt{\frac{12(1-\upsilon^2)}{k}}\sqrt{\frac{F_y}{E}} \tag{7}$$

Here, t is the thickness of plates, b is the width of the plates and K is the buckling coefficient of the plates (4 for 4 side-supported compression members).

Analysis Variables

Establishment of Loading Method

First, to obtain the rate of strain, a lateral load was applied and slowly increased with the fixed central axial load of $0.2P_{cu}$. Then, various values of relative displacement in the perpendicular direction of the member of Fig.2 were set successively with the 0.2 P_{cu} of axial load applied on the loading node. As shown in Fig. 4, the pattern of the cyclic load was determined as follows; (a) the LL type, increasing load in one direction within the tension zone; (b) the CD type, alternation displacement load of constant strain(Δ/l=0.09) in the tension zone; (c) the RD type, alternation displacement load of increasing strain(Δ/l =0.01, 0.03, 0.06, 0.09) in the tension and compression zone.

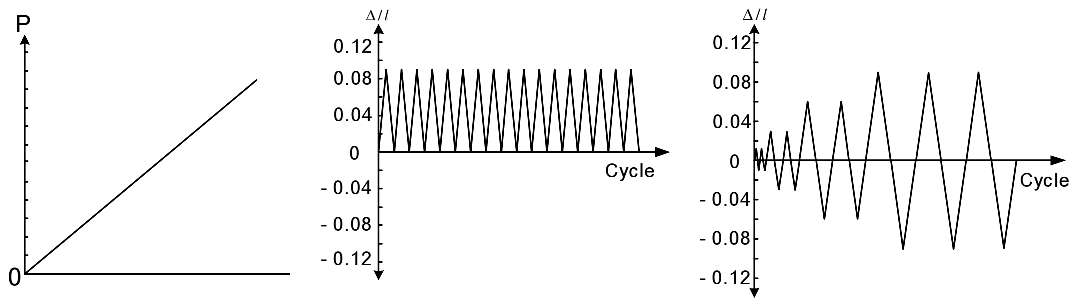

(a) LL Type (b) CD Type (c) RD Type

Fig. 4 Loading Patterns

Model Settings according to Steel Type

In this study, the analysis was performed for the various steel types and loading patterns. The steel types used here are the SS400, which is a standard-strength cold drawn steel for structures and the high-strength Posten80. For each steel type, the following types of loads were applied with the fixed central axial load of $0.2P_{cu}$: the LL type, increasing load in one direction within the tension zone; the CD type, alternation displacement load of constant strain in the tension zone; the RD type, alternation displacement load of increasing strain in the tension and compression zone. Then non-linear analysis was carried out to compare and analyze the damage process and failure behavior. Table. 3 summarizes the variables used in this analysis.

Table. 3 Parameters for Analysis

Specimen	Material Type	Loading Patten
US40-32-69-LL	SS400	LL
US40-32-69-CD	SS400	CD
US40-32-69-RD	SS400	RD
US80-44-95-LL	Posten80	LL
US80-44-95-CD	Posten80	CD
US80-44-95-RD	Posten80	RD

RESULTS AND DISCUSSIONS

Steel Members Subject to Lateral Load

Fig. 5 and 6 show the distribution of the displacement(Δ) in the lateral direction and the strain in the longitudinal direction. It can be noted that the lateral strain of the steel members that are subject to lateral loads increases abruptly after the element reaches the yielding point. There are two factors that are responsible for this phenomenon. First one is the expanded lateral force. The other factor is the expansion of the plasticity zone which is the result of stress redistribution. This is because the displacement increase effect is amplified as the number of elements that are in the plasticity zone increases.

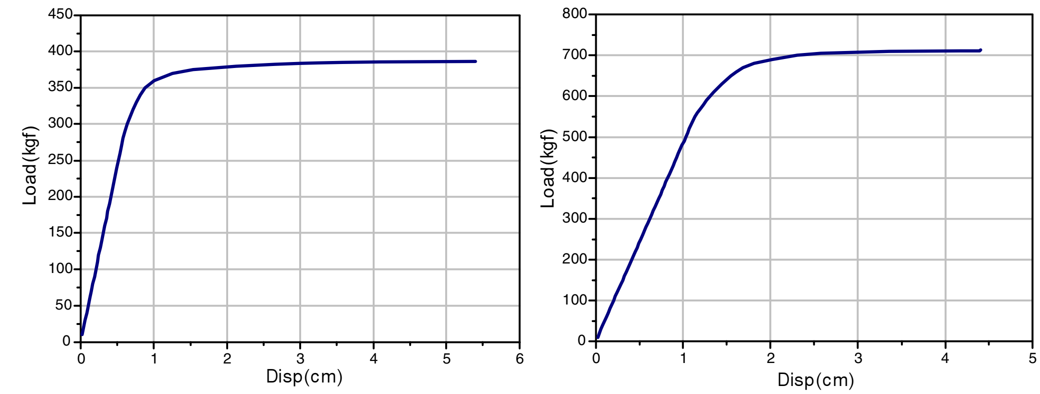

US40-32-69-LL US80-44-95-LL

Fig. 5 Load-Displacement Curves under LL-type loading

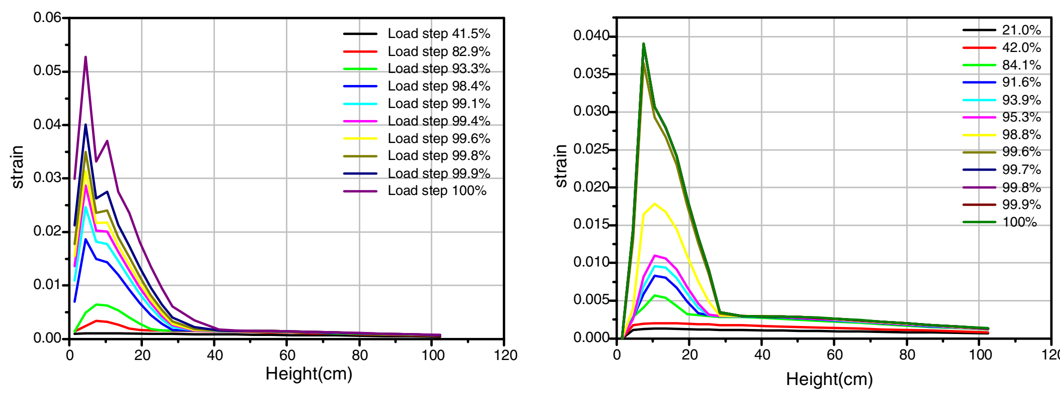

US40-32-69-LL US80-44-95-LL

Fig. 6 Strain Distribution Curves under LL-type loading

Steel Members under Alternating Displacement

Each picture in Fig. 7 shows the relationship between the local stress and strain at 0.045h, 0.11h and 0.67h of the plain that is subject to compressive load. The maximum cumulative plastic strain occurred at 0.45h regardless of the steel type or loading conditions used. For the SS400, maximum strain was 0.27 and 0.21 under the CD and RD loading conditions respectively. Conversely, the Posten80 showed the maximum strain of 0.26 under the RD loading condition, which is larger than the value from the CD loading condition (=0.20).

As for the change of the strain that corresponds to the variation of the loading condition and height of the measurement, the type of a steel is supposed to affect the change of the strain with respect to the variation of the loading condition. This characteristic becomes more apparent for the Posten80, which has a higher yielding strength.

In the case of the high-strength Posten80, the rate of increase in plastic deformation at each element became slower with the repetition of the load for both of the loading conditions. Also, the strain distribution at the height of the member was not significantly affected by the types of loading conditions. Conversely, the result of the SS400 shows substantial variation according to the types of loading patterns. In the CD loading condition, the rate of increase in plastic deformation did not vary significantly with the successive increase of load. Different from the Posten80, the element at 0.67h showed only the elastic behavior. In the RD loading condition, the rate of increase in plastic deformation got slower with the successive increase of load, and the plastic behavior was observed up to 0.67h of the measurement height.

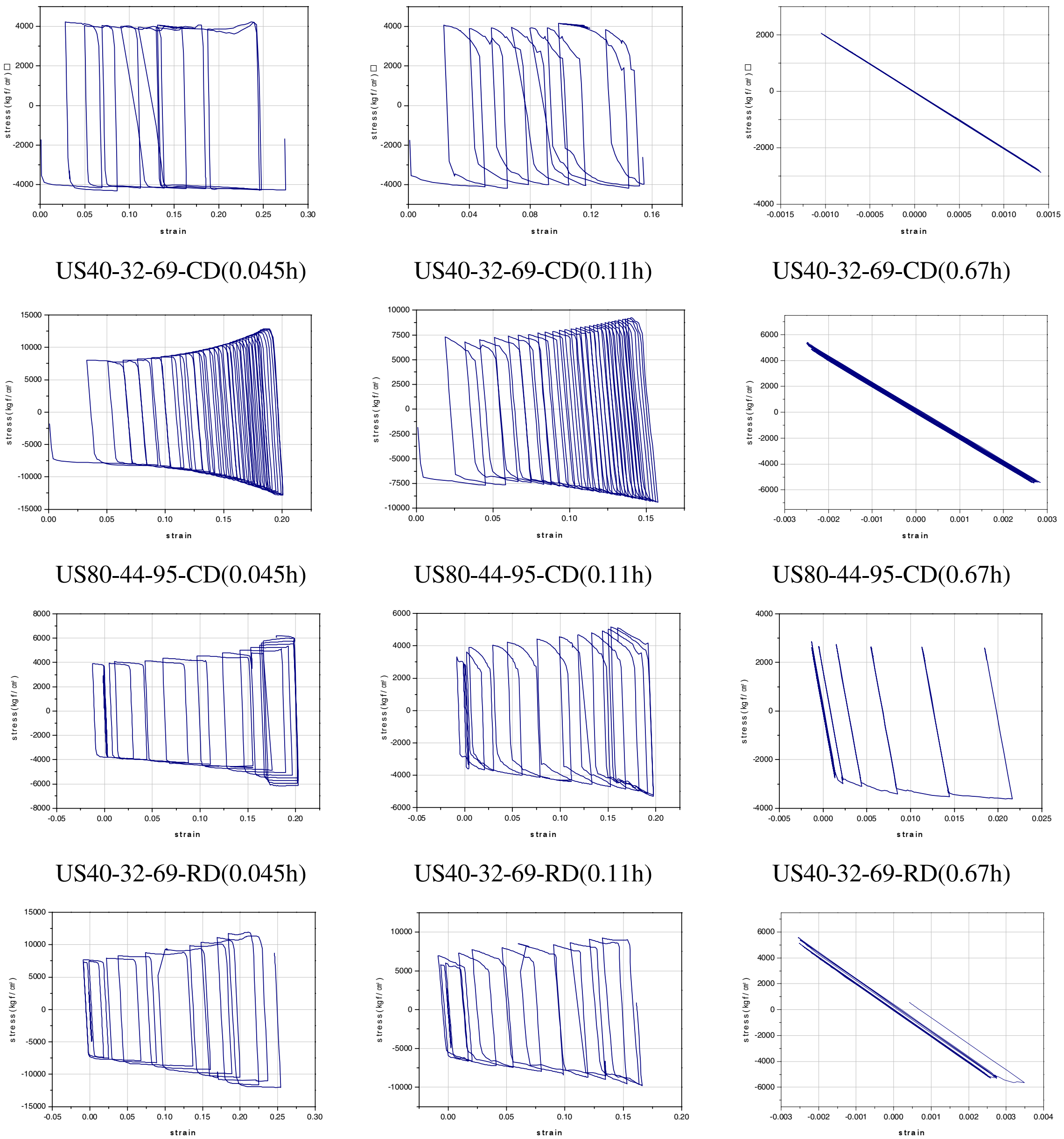

US40-32-69-CD(0.045h) US40-32-69-CD(0.11h) US40-32-69-CD(0.67h)

US80-44-95-CD(0.045h) US80-44-95-CD(0.11h) US80-44-95-CD(0.67h)

US40-32-69-RD(0.045h) US40-32-69-RD(0.11h) US40-32-69-RD(0.67h)

US80-44-95-RD(0.045h) US80-44-95-RD(0.11h) US80-44-95-RD(0.67h)

Fig. 7 Local Stress-Strain Curves under RD, CD-type loading

DAMAGE EVALUATION FOR EACH MODEL

Fig. 8 displays the cumulative maximum strain at each measurement height for the successive increase of the load. For both the Posten80 specimens, such as the US80-44-95-CD and the US80-44-95-RD, plastic deformation occurs up to 0.6h of the member height. However, the plastic deformation for the SS400 specimen US40-32-69-CD occurs up to 0.5h of the member height, while the other SS400 US40-32-69-RD has a larger range of plastic deformation up to 0.7h. From this, it can be noticed that plastic deformation occurs within a similar range for high strength steel members regardless of the loading condition. On the other hand, it can be also noted that the range at which plastic deformation occurs is large for the low-strength steel members under the repetitive loading of compression and tension.

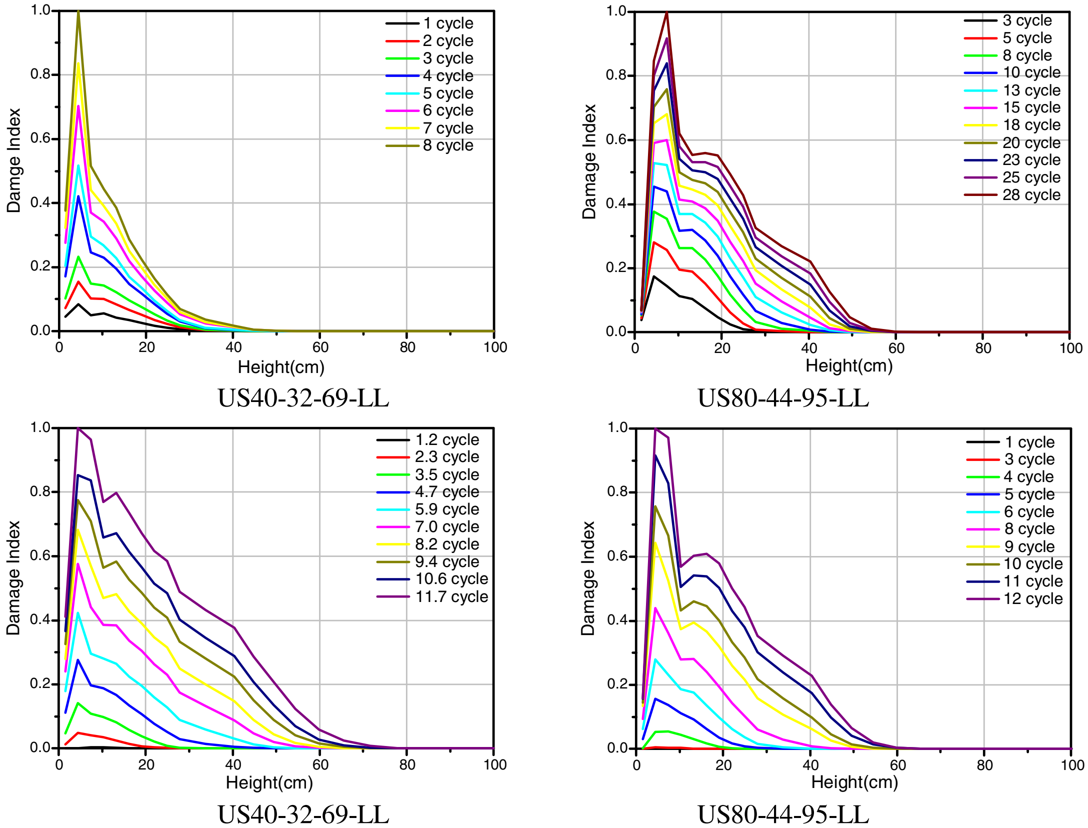

Fig. 8 Damage Index Curves by Loading Cycles

One of the characteristics of cumulative strain curves for the Posten80 specimens is that the maximum cumulative plastic strain occurred at 0.045h regardless of the type of load applied. Furthermore, the behavior of the cumulative plastic strain for the portion that is higher than the failure of a member is similar for both of the loading conditions. Conversely, the SS400 specimen with the RD loading pattern showed a larger range plastic strain, which is a result of stress redistribution for the portion that is higher than the failure. The SS400 specimen with the CD loading pattern did not the show high stress-redistribution effect, and the failure occurred at a relatively low cycle of the load (=9). This result reveals the fact that low-strength steel is highly vulnerable to loading patterns such as the repetitive load of compression. Thus, it can be ascertained that the characteristics of plastic strain is similar for high strength steel members regardless of the pattern of the load applied, while the low strength steel members show different behaviors of the plastic strain for the different patterns of the cyclic load.

The damage evaluation method that was suggested in this study was applied to this model. The US40-32-69-CD showed a sudden increase of the damage index around the 4th cycle of the loading pattern, reaching the index value of 1 around the 9th cycle of the loading. The US40-32-69-RD showed a gradual increase of damage index reaching failure around the 11.7th cycle of the loading. The US80-44-95-CD also showed a gradual increase of damage index up to the 15th cycle of the loading, then the growth of the damage index got slower reaching the failure around the 28th cycle of the loading pattern. The behavior of the US80-95-RD was similar to the one of the US40-32-69-RD.

CONCLUSIONS

This study suggested equations for the damage index, and examined the behavior of steel members that are subjected to cyclic loads using the damage index. Also, the non-linear structural analysis was performed using variables such as loading patterns and types of steel. The results of this study are as follows.

(1) The damage index, which can quantify the degree of damage of the steel members under severe cyclic loads, can be represented with the following equation

$$D = \sum_{i=1}^{n} \left(\frac{\varepsilon_i}{\varepsilon_{\lim}}\right)$$

(2) Using the property values that are obtained from the material test, the finite element analysis was performed to investigate the local strain of the steel members when they fail. The local maximum strain of the SS400, which is a standard-strength cold drawn steel for structures, was 150% at the rupture. Also, the SS400 showed strain distribution because of the stress redistribution effect. The local maximum strain of the high-strength Posten80 was 130% at the rupture, and it barely showed stress distribution.

(3) The plastic strain of high strength steel material occurs within a similar range regardless of the pattern of the load, while low strength steel material shows a larger range of plastic strain during a loading pattern of repetitive tension and compression. Furthermore, the characteristic of cumulative plastic strain was similar for high strength steel regardless of the pattern of the load. Conversely, the behavior of the cumulative plastic strain for the low strength steel was strongly affected by the pattern of the load.

(4) Through the comparison using the damage evaluation method, it could be noted that the loading pattern does not significantly affect the damage on the high strength Posten80, while the low strength SS400 was vulnerable to the loading pattern of repetitive compression.

ACKNOWLEDGEMENTS

This study has been supported by KOSEF(Korea Science and Engineering Foundation)(Subject Number R01-2001-000-0484-0(2003))

REFERENCES

1. Aslani F, Goel SC. “Stitch spacing and local buckling in seismic-resistant double-angle braces.” J. Struct. Engrg., ASEC, 117(8), 1991 : 2442-2463.
2. Hanbin Ge. “Cyclic tests of concrete-filled steel box columns”, Journal of Structural Engineeing ASCE/October 1996 : 1169-1177.
3. Iwai S, Nonaka T, Bourgund U, Kameda H. “Structural failure due to very low-cycle fatigue of steel members and elements under earthquake loading.” Proc., 8th Japan Earthquake Engrg. Symp., 2, 1990 : 1377-1382.
4. Lizhi Jiang, Yoshiaki Goto, Makoto Obata. “Multiple spring model for 3D-hysteretic behavior of thin-walled circular steel piers”, Structural Eng./Earthquake Eng. JSCE/Vol.18 No.2, 2001 : 111s-127s.
5. Shengbin Gao, Tsutomu Usami. “Eccentrically loaded steel columns under cyclic in-plane loading”, Journal of Structural Engineering/August, 2000 : 964-972.
6. Bannantine JA, Comer JJ, Handrock JL. “Fundamentals of metal fatigue analysis”, Prentice-Hall Inc., 1990.
7. Chopra AK. “Dynamics of structures theory and applications to earthquake engineering”, Prentice Hall., 1995.
8. Crisfield MA. “Non-linear finite element analysis of solids and structures”, Volume 1, John Wiley & Sons Ltd., 1997.
9. Crisfield MA. Non-linear finite element analysis of solids and structures, Volume 2, John Wiley & Sons Ltd., 1997.

10. MSC/NASTRAN. “Non-linear analysis”, The Macneal-Schwendler Corporation, 1992.
11. Nonaka T, Iwai S. “Failure of bar structure under repeated loading.” Structural Failure, T. Wierzbicki and N. Jones, eds., John & Sons, New York, N.Y., 1998 : 398-433.
12. Park YS. “Damage process of steel members under very-low-cycle loading”, Dissertation of Civil Engineering Department, Kyoto University, 1993.
13. Yamada M. “Low Cycle Fatigue Limits of Various Kinds of Structural Members subjected to Alternately Repeated Plastic Bending under Axial Compression as an Evaluation Basis or Design Criteria for Aseismic Capacity” Proc. of 4th World Conference on Earthquake Engineering, Vol. 1, 1963 : 137-151.